CHAPTER II
LITERATURE REVIEW

2.1 CANDU Primary Coolant Loop

The CANDU reactor uses a fission-controlled reaction like all other nuclear power reactors. However, the CANDU reactor is fuelled with natural uranium (UO_2) sheathed with Zircaloy. The fuel is contained in the 380 pressure tubes made of Zr 2.5% Nb. Heat from the nuclear reaction is removed by heavy water (D_2O), which is the primary coolant. The generated heat is carried by the reactor coolant through carbon steel pipes and headers to the steam generator. The steam generator contains nickel tubes. The secondary side light water is converted into saturated steam by heat transferred from the primary coolant. The primary coolant is returned through the feeder inlet pipes to the reactor core. The pressure tubes in the reactor core are connected to feeder pipes via end fittings that are designed for convenient re-fuelling. A Grayloc hub is used to attach each feeder to its fuel channel end fitting. The reactor coolant circulation is called the primary coolant system as shown in Figure 2.1.

The CANDU primary coolant loop consists of three main components: the steam generator, the reactor core and the piping system. The material of construction of each component is shown in the following table.

Table 2.1 Material constructions

Component	Materials Used
Reactor core	Zirconium alloy 2.5%Nb
Steam generator*	Nickel alloy - Monel 400 - Inconel 600 - Incoloy 800
Piping	A-106 Grade B Carbon Steel

*Depends upon the CANDU model

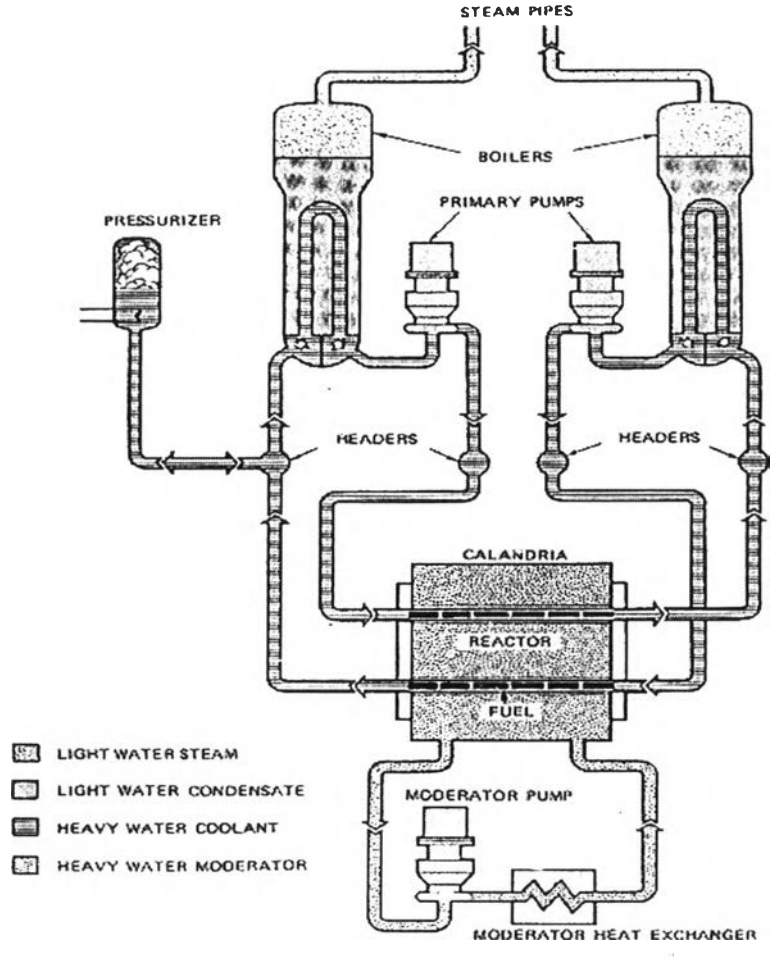

Figure 2.1 Primary coolant system of CANDU reactor (Silpsrikul, 2001).

The primary coolant D_2O enters the core at 265 °C and leaves at 310 °C with the steam quality ranging up to 6%. The steam quality increases slightly in transit because of the pressure drop along the piping. Average linear velocities of the coolant in the outlet feeders range from 8.0 m/s to 16.5 m/s. Chemicals are added to the coolant flow for two major requirements: 1.) to minimize dissolved oxygen by dissolving hydrogen within the specification of 3-10 cm^3/kg at STP and 2.) to maintain the alkalinity by adding lithium hydroxide to within the specification of pH of 10.3 to 10.8 at room temperature (Lister *et al.*, 1998).

2.2 Corrosion Mechanisms

Corrosion is the destructive result of electrochemical reaction between a metal or metal alloy and its environment (Jones, 1992).

The corrosion of metals in an aqueous system involves two or more electrochemical reactions. Carbon steel corrosion can be represented by two simple reactions as the following

Anodic reaction: $Fe \rightarrow Fe^{2+} + 2e^-$ (2.1)

Cathodic reaction: $2H_2O + 2e^- \rightarrow H_2 + 2OH^-$ (2.2)

Iron metal is corroded and converted to iron ions, ferrous (Fe^{2+}), formed at the anodic surface. In deaerated solution, hydrogen molecules are formed at the cathodic surface.

The cathodic reaction can be accelerated by dissolved oxygen into the solution, a process called depolarization according to the following reaction:

$$O_2 + 2H_2O + 4e^- \rightarrow 4OH^- \quad (2.3)$$

The oxidation proceeds rapidly as oxygen molecules reach the iron surface.

By adding reaction (2.1) and (2.3), the corrosion product will be formed as follows

$$Fe + H_2O + 1/2O_2 \rightarrow Fe(OH)_2 \quad (2.4)$$

Ferrous hydroxide, $Fe(OH)_2$, forms the diffusion barrier layer next to the iron surface through which O_2 must diffuse.

Berge *et al.* (1976) proposed the reaction that accompanies the formation of magnetite by water as written below.

$$3Fe + 4H_2O \rightarrow Fe_3O_4 + 4H_2 \quad (2.5)$$

Sanchez *et al.* (1998) stated that ferrous hydroxide produced in the first step can form magnetite according to the reaction

$$3Fe(OH)_2 \rightarrow Fe_3O_4 + H_2 + H_2O \quad (2.6)$$

The ferrous hydroxide can transform into magnetite in high temperature water, above 100°C, by the Schikorr reaction. The reaction increases with increasing temperature (Berge *et al.*, 1976).

$$3Fe(OH)_b^{(2-b)+} + (4-3b)H_2O \rightarrow Fe_3O_4 + 3(2-b)H^+ + H_2 \quad (2.7)$$

If the system is unsaturated, magnetite (Fe_3O_4) can dissolve through the reverse Schikorr reaction that leads to the following species: Fe^{2+}, $Fe(OH)^+$, $Fe(OH)_2$, $Fe(OH)_3^-$ depending on the pH of the system (Lang, 2000). Figure 2.2 shows the predominant species of iron ions as a function of temperature. Obviously, $Fe(OH)_2$ is the dominant one at 300 °C or $pH_{25°C}$ of 10, which are the operating conditions of the primary coolant loop system.

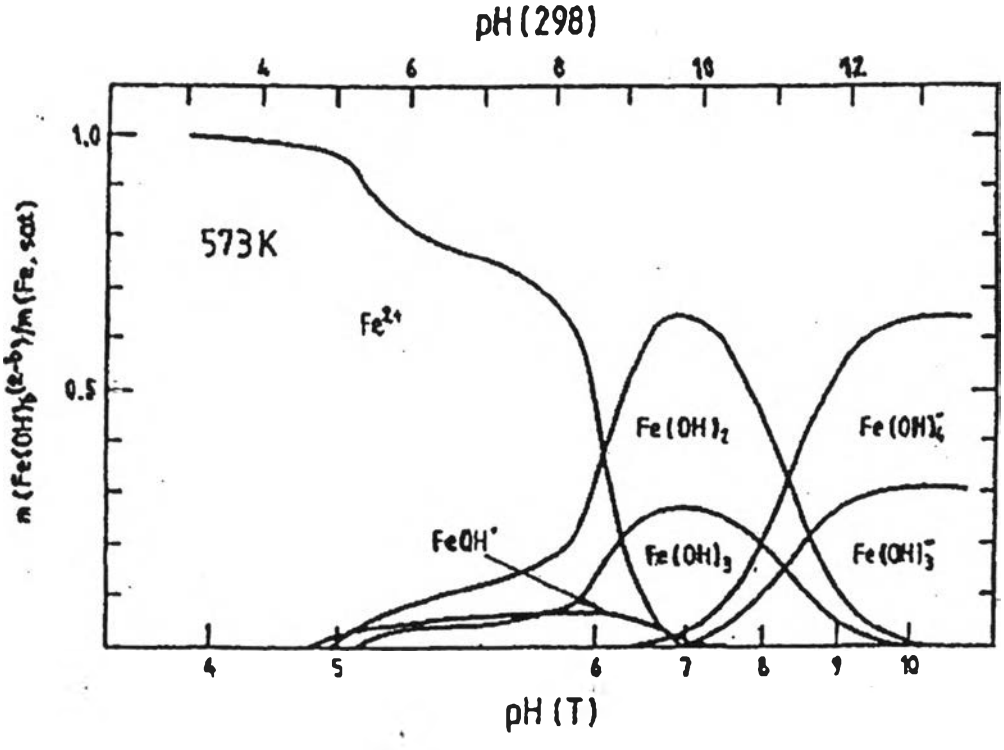

Figure 2.2 Predominant species diagram at 300 °C (Tremaine and Leblannc, 1980).

Cheng and Steward (2004) reported that a hydrous $Fe(OH)_2$ layer is formed on the steel surface by the following mechanisms.

$$Fe + H_2O \rightarrow Fe(OH) + H^+ + e^- \quad (2.8)$$

$$Fe(OH) \rightarrow Fe(OH)^+ + e^- \quad (2.9)$$

$$Fe(OH)^+ + OH^- \rightarrow Fe(OH)_2 \rightarrow \text{hydrous } Fe(OH)_2 \quad (2.10)$$

At temperatures above 150 °C, the poly-condensation will occur and change the $Fe(OH)_2$, to FeO. However, FeO is unstable in water and changes to magnetite and generates hydrogen.

$$Fe(OH)^{+} + Fe(OH)_2 + e^{-} \rightarrow Fe\text{-}O\text{-}FeOH \rightarrow (FeO)_n \text{ condensation} \quad (2.11)$$

$$3FeO + H_2O \rightarrow Fe_3O_4 + H_2 \quad (2.12)$$

Therefore, it can be concluded that in high temperature water, corrodes and forms an oxide film, Fe_3O_4, covering the metal surface.

2.3 Mechanism of Oxide Film Growth

A considerable number of investigations have been devoted to the study of the formation mechanism of a passive film. It is generally accepted that the corrosion of carbon steel and low alloy steel, in the absence of oxygen, involves the inward diffusion of oxygen bearing species to the metal/oxide interface and the outward diffusion of the iron ions to the solution. When iron ions pass into the solution, it becomes saturated with dissolved iron. The outer oxide layer will be formed as an outer oxide layer by precipitation and growth on the inner oxide layer.

In high temperature water, the diffusion through the existing oxide layer is by short circuit routes such as micro-pores and grain boundaries, rather than the lattice. Therefore, in the absence oxygen as in the primary system of CANDU reactors, the possible oxygen bearing species might be either water molecules, oxygen ions or hydroxide ions diffusing along the short circuit routes.

Cheng and Steward (2004) stated that the oxygen bearing species involving the formation of the magnetite film should mainly be water which acts as a binder between oxide chains because oxygen ions will involve the formation of the oxide film only after a sufficiently anodic potential is applied and a de-protonation of water takes place. Hydroxide ions are not likely to be the diffusing species due to the electrical charge strength across the thin film which is high, results in the blocking of the negative species, the hydroxide ion, which moves toward to the metal surface.

Hydrogen ions are formed from the Schikorr reaction as shown in reaction (2.7). Hydrogen ions diffuse inward through the oxide film to neutralize the electrons from anodic reactions and form as H_2 at the metal/oxide interface. Diffusion of hydrogen ions through the oxide film is driven by the concentration and electric potential gradient. It is expected that hydrogen ions diffuse through the oxide film relatively slowly because the ionic crystalline oxide has a low hydrogen

diffusion coefficient and thus, provides a definite resistance to hydrogen. However, Tomlinson (1981) proposed that the diffusion of hydrogen ions through the lattice should take place without physical hindrance because the size of the hydrogen ions is small (~10^5 times smaller than other ions) and similar in size to electrons.

The iron ions generated by the anodic dissolution reaction of steel are immediately formed as an inner oxide layer at the metal/oxide interface. The remainder of the dissolved iron diffuses outward through the oxide layer and forms an outer oxide layer at the oxide /solution interface. The schematic diagram of the magnetite film formed on a steel surface in high temperature water is shown in the Figure 2.3.

At the steel/oxide interface, iron dissolves into the solution when no oxide layer exists. Water molecules diffuse through the inner oxide layer and directly react with the metal surface resulting in the formation of the magnetite film or as an inner oxide layer. Hydrogen ions from the water solution can also diffuse inward through the oxide layer under the concentration and potential gradient and form hydrogen atoms at the steel/oxide interface. Tomlinson (1981) reported that up to 90% of the hydrogen atoms are formed at the steel/oxide interface and more than 99 % probably diffuse through the metal at the temperature of interest.

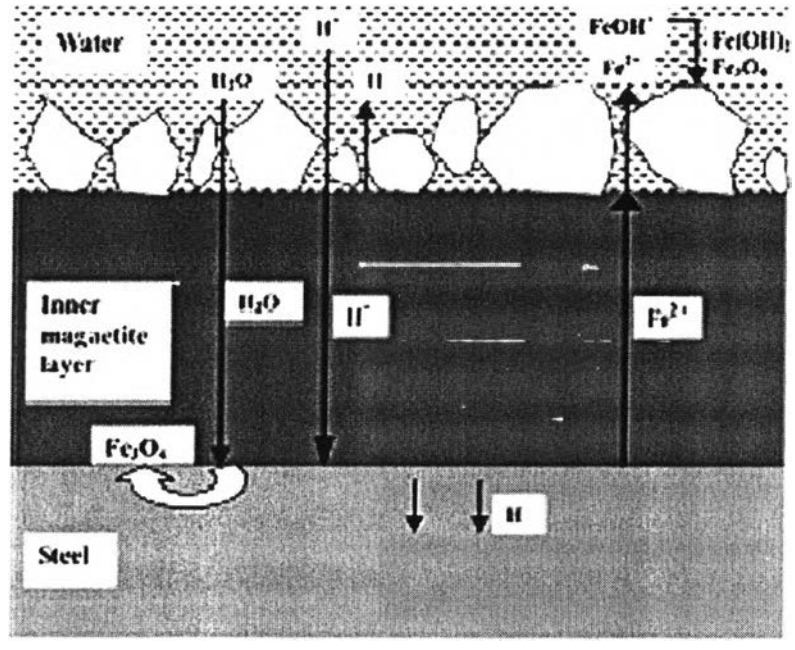

Figure 2.3 Schematic diagram of the formation mechanism of magnetite on the steel surface in high temperature water (Cheng and Steward, 2004).

At the oxide/solution interface, the remainder of the iron ions diffuse through the inner oxide layer as $Fe(OH)^+$. For high temperature water, $Fe(OH)^+$ will change to FeO, an unstable species, and react with water to form an outer oxide layer according to the Schikorr reaction (2.7). Robertson (1989) and Lang (2000) stated that the outer layer can dissolve in the fluid, depending on the water chemistry. At the same time, hydrogen ions can also be produced by the Schikorr reaction and diffuse through the inner oxide layer.

2.4 Oxide Film Characterization

The morphology of the oxide film is influenced by the chemical composition of the alloy, exposure conditions and surface finishing. Magnetite (Fe_3O_4) is one structure of iron oxide that is observed on a metal surface such as carbon steel in CANDU reactors (Lister *et al.*, 1994). It behaves like a corrosion resistance film to protect the steel matrix from the corrosive environment. As

mentioned in the former section, it consists of double layers, and is called a duplex of magnetite or Potter and Mann layer (Potter and Mann, 1962).

1) Inner oxide layer: The morphology of this layer is small crystals, compact and adherent because it nucleates in the confined space and grows at the metal/oxide interface, replacing the corroded volume (Potter and Mann, 1962).

2) Outer oxide layer: The morphology of this layer is coarse octahedral crystals since it grows outward without volume constraint.

The structure of magnetite (Fe_3O_4) is an inverse spinel. The unit cell of the normal spinel consists of $32O^{2-}$, $8Fe^{2+}$ and $16Fe^{3+}$. For inverse spinel, one half of Fe^{3+} occupy tetrahedral sites and the rest are arranged with the Fe^{2+} at random in the 16 octahedral positions, and are based in a cubic close pack sublattice of O^{2-}.

There have been extensive studies about the morphology of oxide films on austenitic stainless steels in high temperature water. It was generally accepted that the oxide layer of stainless steels also consists of a double layer.

Lister *et al.* (1987) reported the inner oxide, amorphous, layer of 304L stainless steel was a chromium-rich spinel $Ni_xCr_yFe_{3-x-y}O_4$ with non-stoichiometry composition under high temperature alkaline water, reducing conditions. Different values were reported for x and y with Fe_2CrO_4, $FeCr_2O_4$ and $NiCr_2O_4$ as a limiting case. The inner oxide layer was always enriched in chromium and depleted in nickel. This can be explained by preferential dissolution of Fe and Ni during passivation and to the low diffusivity and solubility of chromium in spinel lattice. The metal diffusion rate can be ranked approximately as Mn > Fe > Co > V > Ni > Cr (Robertson, 1989). While, the outer oxide, crystalline, layer will be octahedral magnetite containing nickel, presumably iron-rich spinel with the non-stoichiometry structure $Ni_xFe_{3-x}O_4$.

Kim (1994) studied the effect of high temperature water chemistry on the morphology and chemical structure of the 316 stainless steel oxide films under normal water conditions (NWC), 200 ppb O_2 and 20 ppb H_2 and hydrogen water conditions (HWC), 150 ppb H_2 and 15 ppb O_2. The results showed that the existing outer oxide layer composition depended upon the water chemistry. A closely packed, thicker oxide with small particle size was formed under NWC conditions, while a less packed oxide with a large particle size was formed under HWC conditions, while the inner oxide layer remained unaffected.

2.4.1 pH Effect

Stainless steel is valuable not only because of its low corrosion rate but also because the low rates extend over a wider range of pH compared to carbon steel. Particularly, the improvement is marked in acid chloride solutions, where carbon steel undergoes non-protective corrosion, while stainless steels are able to maintain protective corrosion, with consequently much lower corrosion rates. The non-protective corrosion of carbon steels arises because an acid chloride solution induces porosity in its magnetite film. The porosity allows the solution access to the metal/oxide interface easily so that the corrosion rate is limited by an interfacial reaction rather than being diffusion controlled. In contrast, stainless steel containing over 3% Cr is able to maintain a low porosity oxide, so the corrosion rate remains diffusion controlled.

The pH value also affects the solubility of the magnetite (Fe_3O_4) film. Tremaine and LeBlanc (1980) studied the effect of pH and temperature on Fe_3O_4 solubility. The $pH_{25°C}$ of approximately 10.5 gave the lowest solubility of Fe_3O_4 as shown in Figure 2.4

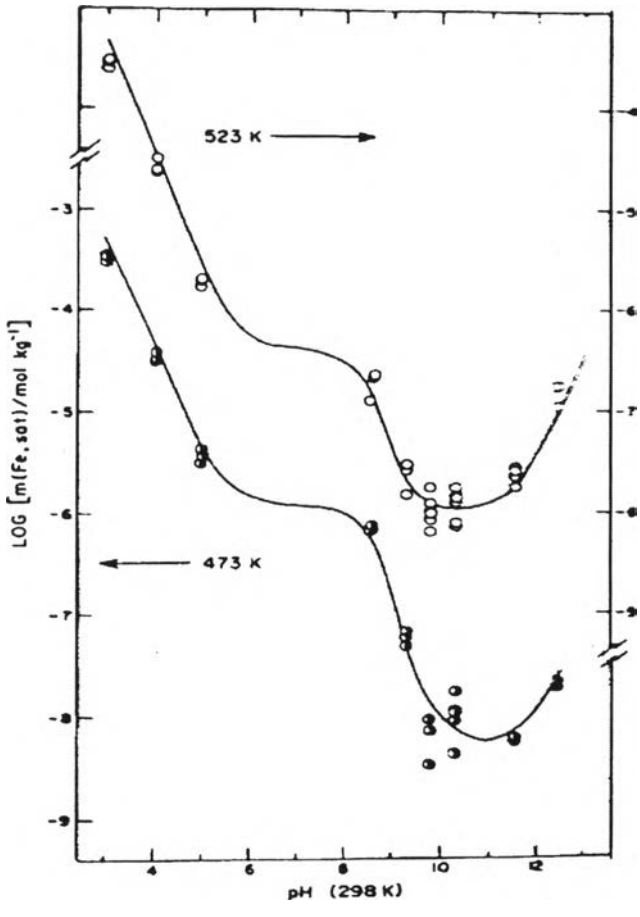

Figure 2.4 Experimental Solubility at 523 K and 473 K plotted against the initial pH of the feed solution (Tremaine and LeBlanc, 1980).

2.4.2 Dissolved Oxygen Effect

Appreciable corrosion of iron or steel at ordinary temperatures requires dissolved oxygen in neutral and alkaline solutions. Since the cathodic reaction can be accelerated by dissolved oxygen and its diffusion rate at steady state is proportional to oxygen concentration that follows reaction (2.3), the corrosion rate is proportional to the oxygen concentration. A protective magnetite film is stable in the absence of dissolved oxygen. Therefore, any factors affecting the amount of dissolved oxygen will affect the corrosion of steel proportionally such as agitation or stirring that increases transport of dissolved oxygen and consequent corrosion rate.

Kim (1996) studied the effect of different water chemistries on the chemical structure, composition and thickness of the 304L stainless steel oxide film in 288 °C water. He found that at high electrochemical corrosion potential (ECP) with O_2 rich water, Cr tends to dissolve into the solution as chromate (CrO_4^{2-}) therefore a Cr deficient oxide is expected to be form as follow.

$$(Ni, Fe)\ Cr_2O_4 + 3/2O_2 + H_2O \rightarrow (Fe^{2+}, 2Ni^{2+}) + 2\ Cr_2O_4^{2-} + 2H^+ \qquad (2.13)$$

The smaller particles formed a closely packed and thicker film, compared to oxide film formed in H_2 water chemistry under reducing conditions (See Figure 2.5). The outer oxide structure is hematite (α-Fe_2O_3), but the inner oxide structure is $FeCr_2O_4$, the same as the one formed in H_2 chemistry.

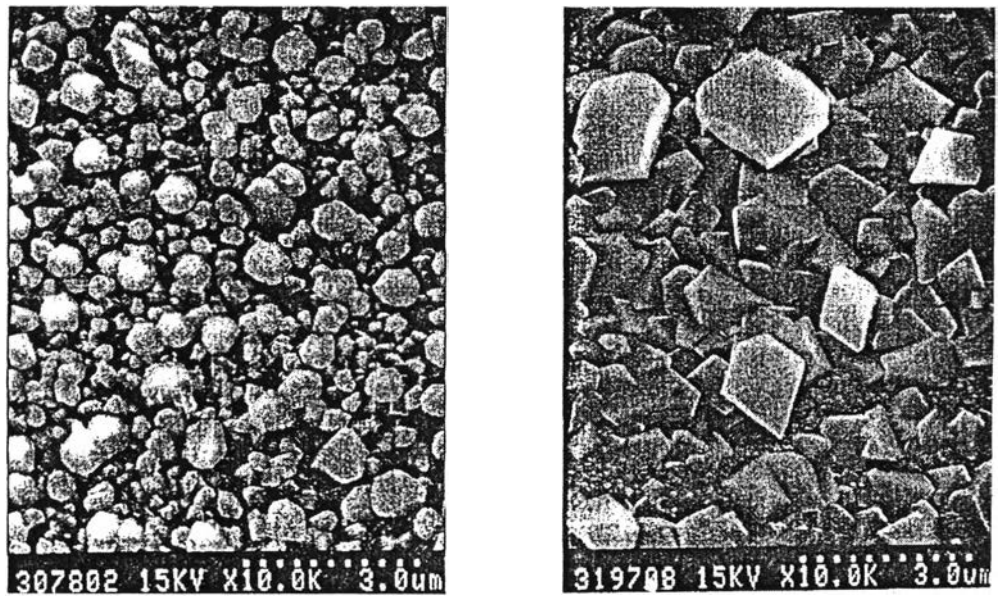

(a) (b)

Figure 2.5 SEM pictures showing the oxide surface formed on type 304SS at 288 °C: (a) under O_2 and (b) H_2 water chemistry (Kim, 1996).

2.4.3 Hydrogen Effect

Hydrogen can migrate readily through the crystal structure of most metals and alloy, including pure iron and carbon steels. Hydrogen damage includes a number of detrimental effects on metallurgical and mechanical properties. Initial hydrogen entry can result in loss of ductility and brittle cracking and additional

hydrogen can nucleate to form as hydrogen gas, which forms internal voids and surface blisters. Hydrogen can be made available to a metal surface from various sources, including the cathodic reaction of hydrogen or water according to reaction (2.2).

Moreover, hydrogen may also enter the metal from hydrogen-bearing atmospheres during heat-treating, welding, or other manufacturing processes. Water vapor and steam may be decomposed to hydrogen at hot surfaces during welding or heat treatment.

According to the Schikorr reaction, it is found that the hydrogen concentration affects the amount of $Fe(OH)_b^{(2-b)+}$ in the system. The equilibrium constant can be written as

$$K = \frac{\left[Fe(OH)_b^{(2-b)+}\right]}{\left[H^+\right]^{2-b}\left[H_2\right]^{1/3}} \qquad (2.14)$$

If the pH is constant, equation (2.14) can be rewritten as

$$K' = \frac{\left[Fe(OH)_b^{(2-b)+}\right]}{\left[H_2\right]^{1/3}} \qquad (2.15)$$

From (2.15), it is indicated that the concentration of ferrous species increases with increasing hydrogen. This means the local solubility of magnetite increases with the power 1/3 of H_2 concentration and is confirmed by Berge *et al.* (1976).

Kim (1996) reported that at low ECP in H_2 rich water, Cr tends to concentrate in the oxide film, but Fe becomes more soluble as more ferrous ions (Fe^{2+}), are formed in solution by

$$(Ni, Fe)\,Cr_2O_4 + 6H^+ + H_2 \rightarrow (Ni^{2+}, 2Cr^{3+}) + Fe^{2+} + 4\,H_2O \qquad (2.16)$$

Large particles were observed at the outer oxide layer as shown in Figure 2.5. The electron diffraction pattern results shown that the outer oxide structure is composed of Fe_3O_4 and $FeCr_2O_4$. Therefore, the Cr content of the oxide film under reducing conditions is more concentrates than in oxidizing conditions.

2.4.4 Temperature Effect

When the temperature is increased a drastic change in appearance and the properties of oxide films on stainless steels exposed to water can be observed. Stellwag (1998) stated that the breakdown of passivity in high temperature water is related to crystallization of the initially amorphous, thermodynamically metastable, passive film and thus defects. The produced structural imperfections enable a significant increase in mass transport and thus cause local collapse of the film at metal vacancies accumulating at the metal film interface. Long-term exposure to high temperature water therefore results in an oxide double layer with cracks, pores or other bulk imperfection.

In the case of the corrosion rate of steel, an increasing temperature initially enhances the corrosion rate but also reduces solubility of dissolved oxygen. Thus, above 80 °C, the corrosion rate decreases in an open system. This allows oxygen to escape out of the system as shown in the Figure 2.6.

Nevertheless, in a closed system that retains the dissolved oxygen, the corrosion rate increases, above 80 °C. Stringent control of dissolved oxygen to absolute minimum levels is an obvious requirement to control corrosion in closed high-temperature boiler systems (Jones, 1992).

Also, the temperature can affect to the solubility of magnetite films. Regarding with the primary coolant of CANDU reactor, system is the operated at a pH of approximately 10.5 where the solubility increases with temperature. Therefore, the coolant becomes unsaturated after flowing through the reactor core, since the elevation of temperature causes an increase of magnetite solubility. Consequently, the outer oxide layer can dissolved in the bulk coolant, so the outlet feeder pipes are much more susceptible to thinning than inlet feeder pipes.

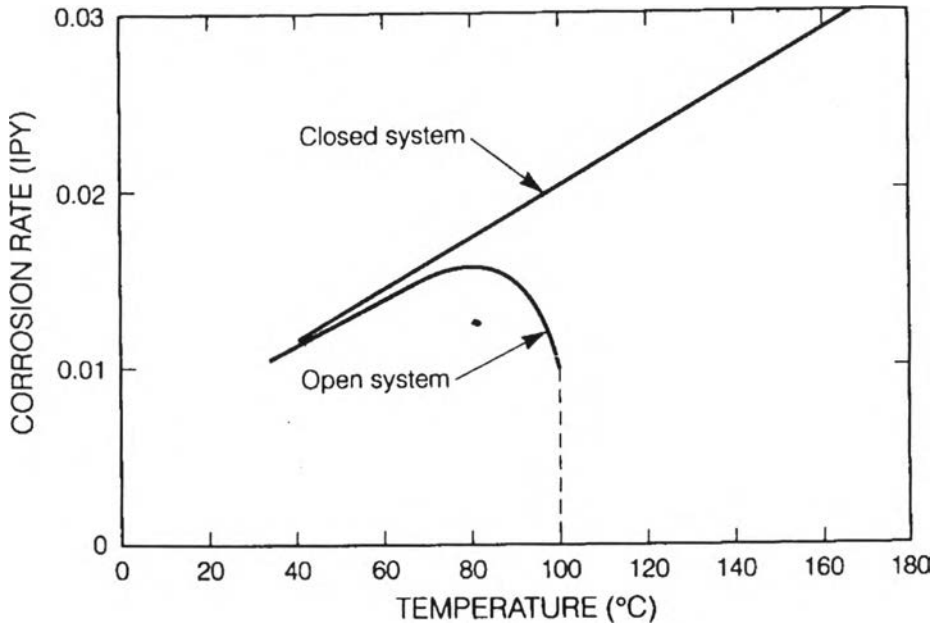

Figure 2.6 Effect of temperature on corrosion of iron in water containing dissolved oxygen (Jones, 1992).

2.4.5 Alloying Effect

Alloying is an effective means for improving the resistance of metals to attack by corrosive environments at either ordinary or elevated temperatures.

Chromium: The outstanding characteristic of high chromium steels is their ability to become passive under suitable conditions and such conditions that provide sufficient oxidizing power to form and maintain a stable oxide film. Fontana (1986) found that the corrosion resistance and heat resistance increased with the nickel and chromium content in the steel. Stellwag (1998) reported that as Cr is added to Fe in an alloy, the oxide film structure changes from polycrystalline to non-crystalline with increasing Cr content and the oxide is perfectly vitreous at chromium content of 24%. Cheng and Steward (2004) found that the formation rate and stability of magnetite film increased with increasing Cr content in the steels as shown in Figure 2.7. The maximum current density and steady state current density decreased with increasing Cr content in the steel.

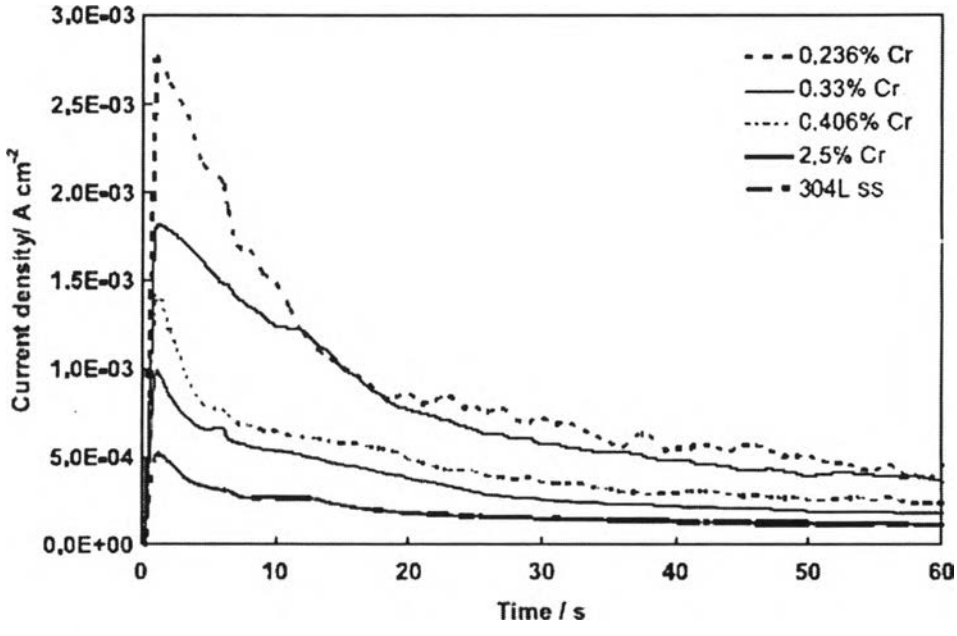

Figure 2.7 Repassivation curves of various steels at -0.79V (SHE) in lithitated solution, $pH_{25°C}$ of 10.6 at 240°C (Cheng and Steward, 2004).

Nickel: In conjunction with chromium improves high temperature oxidation resistance of stainless steels. However, nickel has little effect on oxidation resistance of iron. It also improves resistance to thermal cycling during high temperature oxidation.

Silicon: It forms adherent resistant films alone and in conjunction with chromium. It is added at 2 to 3% levels to many iron and nickel based chromium bearing alloys to improve corrosion resistance, especially at lower temperatures.

Molybdenum: Its influence on corrosion resistance of steel is apparent only when Mo is used in combination with other alloying elements and the Mo content exceeds 3%. The purpose for adding Mo in carbon steel is to increase the strength and hardness.

Carbon: It is an important alloy because the precipitation of carbide reduces the corrosion resistance. The maximum resistance requires that carbide precipitation be suppressed by heat treatment.

Platinum and Palladium: A small amount of both alloys can improves the catalytic efficiency for H_2 and O_2 recombination in high temperature water and thus, decrease the electrochemical corrosion potential of the modified materials.

Tempering can be used to relive strain caused by quenching which can affect the corrosion resistance at high temperatures. As mentioned before, corrosion resistance depends on the chromium content therefore, if chromium combines with carbon to form as carbide then the solid solution is depleted of chromium and consequently gives less corrosion resistance that will occur when tempering temperatures are above 480 °C.

2.5 Flow-Assisted Corrosion (FAC)

Flow-Assisted Corrosion is defined as the acceleration or increase in the rate of deterioration or attack on the metal because of the relative movement between the corrosive fluid and the metal surface. Metal is removed from the surface as dissolved iron, or forms a solid corrosion product that is mechanically swept from the metal surface (Fontana, 1986). It has been confirmed that the water flow velocity plays an important roie in mass transport of the reactants at the surface, and thus produces electrochemical corrosion potential for the materials in such an environment. Heitz (1995) proposed the four mechanisms that describe the conjoint action of flow and corrosion as depicted in Figure 2.8.

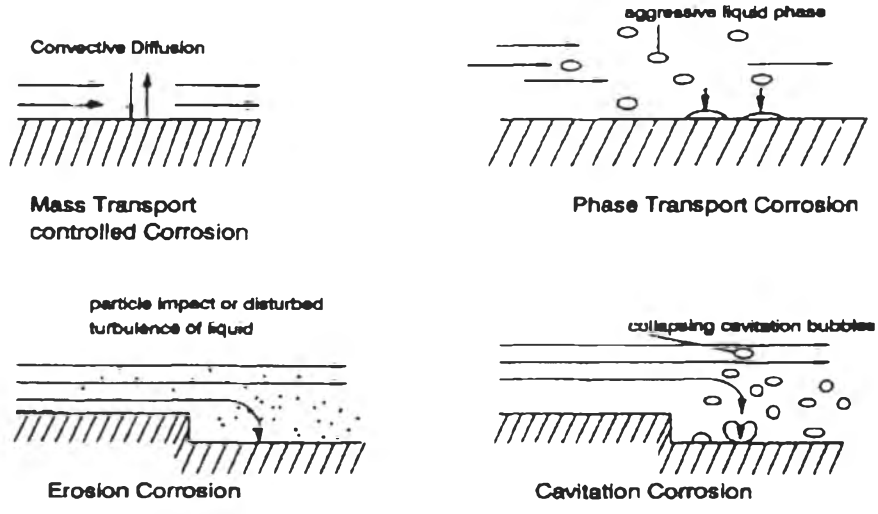

Figure 2.8 Four main mechanisms of flow-assisted corrosion (Heitz, 1995).

Lister *et al.* (1998) explained the effect of FAC on the carbon steel oxide film formed in high temperature water, when the system is saturated with dissolved iron. Under the reducing condition, the oxide film will be mainly composed of Fe_3O_4. FAC can be described by two processes in series: magnetite film dissolution and mass transport of dissolved iron to the bulk coolant. If such a system is under-saturated in dissolved iron, it can cause the dissolution of the oxide layer to the bulk coolant at a rate that depends on the concentration gradient. Mass transport of iron ions to the bulk solution can be increased by increasing the fluid velocity, which results in a higher mass transfer coefficient and the flux of iron ions into the bulk coolant. Therefore, if the mass transfer of iron ions emerging from pores to the bulk coolant is faster than oxide precipitation, no outer layer will form. The FAC effect can be investigated in the primary heat transfer circuit of the CANDU reactor. The outlet feeder pipes undergo more FAC than the inlet feeder pipes, since the coolant temperature of outlet feeder pipe rises from 265°C to 310 °C during flow through the reactor core, where there is no source of iron, resulting in higher solubility of the oxide film. Therefore, the inlet feeder pipes carry the saturated coolant with dissolved iron, which results in lower corrosion rate and a relatively thick oxide film compared with the outlet feed pipes.

2.6 Electrochemistry

As mention in section 2.2, the metal corrosion occurs via electrochemical reactions at the metal and aqueous solution interface. Basically, corrosion processes involve two opposing electrochemical reactions, anodic and cathodic reactions, which can be simply shown as follow

$$Ox + ne^- \longleftrightarrow Re$$

The forward direction is the cathodic reaction while the reverse direction is the anodic reaction. Whenever the rate of the forward reaction (r_f) and reverse reaction (r_r) is identical, means that the system reaches the equilibrium state. From as engineering standpoint, the major interest of corrosion is corrosion rate. The reaction rate (r) can be expressed in term of mass reacted or mass loss per area per time as follow

$$r = \frac{m}{tA} \qquad (2.17)$$

Where r = reaction rate

A = exposed area

t = reaction time

According to Faraday's law, the current can be related to the mass reacted.

$$Q = nFM$$

$$= \frac{nFm}{a} \qquad (2.18)$$

Where Q = charges of transferred electron

n = moles of transferred electron

F = Faraday's constant (96,487 coulombs/mole)

= Charges carried by one mole of electron

M = moles reacted

m = mass reacted (g)

a = atomic weight

The associated charges can be calculated in terms of current (I) and time (t) by Equation (2.19).

$$Q = It \qquad (2.19)$$

Substitution of Equation (2.18) into Equation (2.19) yields

$$m = \frac{Ita}{nF} \tag{2.20}$$

Hence,

$$r = \frac{Ia}{nAF} \tag{2.21}$$

When the rate of anodic and cathodic reactions is equal or no net reaction occurs, the reaction rate is called the exchange reaction rate and the associated current is called the exchange current (I_o), which can be defined by another term as exchange current density or i_o. The exchange current density is the exchange current divided by the exposed area. The equation (2.21) can therefore be arranged to give

$$r_f = r_r = \frac{i_o a}{nF} \tag{2.22}$$

The rate of oxidation and reduction reaction at equilibrium of each electrode can be conveniently represented by the exchange current density (i_o).

In a system that is comprised of different electrochemical electrode potentials corresponding to the different Gibb free energies, one of the electrodes acts as anode and refers to the electrode at which a net oxidation process occurs. Another acts as the cathode electrode at which a net reduction process occurs. Therefore, the potential of these electrodes will be no longer at their equilibrium potential (E_O). This deviation from equilibrium potential is called polarization or equated by $E - E_O$. Polarization can be defined as the displacement of electrode potential resulting from a net current. The magnitude of polarization is frequently measured in terms of overvoltage (η).

Figure 2.9 schematically illustrates the typical behavior of an active-passive metal. The metal initially demonstrates behavior similar to a nonpassivating metal with no oxide film. As the electrode potential is made more positive or higher η, the current density ,which can refer to dissolution rate, will be increase exponentially. This is the active region. At higher potential, the dissolution rate decreases to a small value and remains independent of potential over a considerable potential region because of the formation of the oxide film. This region is the passive region. Finally, the dissolution rate again increases with increasing potential in the transpassive

region. E_{PP} is the primary passive potential where the anodic current density (I_c) is a maximum. If one compares E_{pp} of different materials, a lower value of E_{pp} means it is easier to form the oxide film.

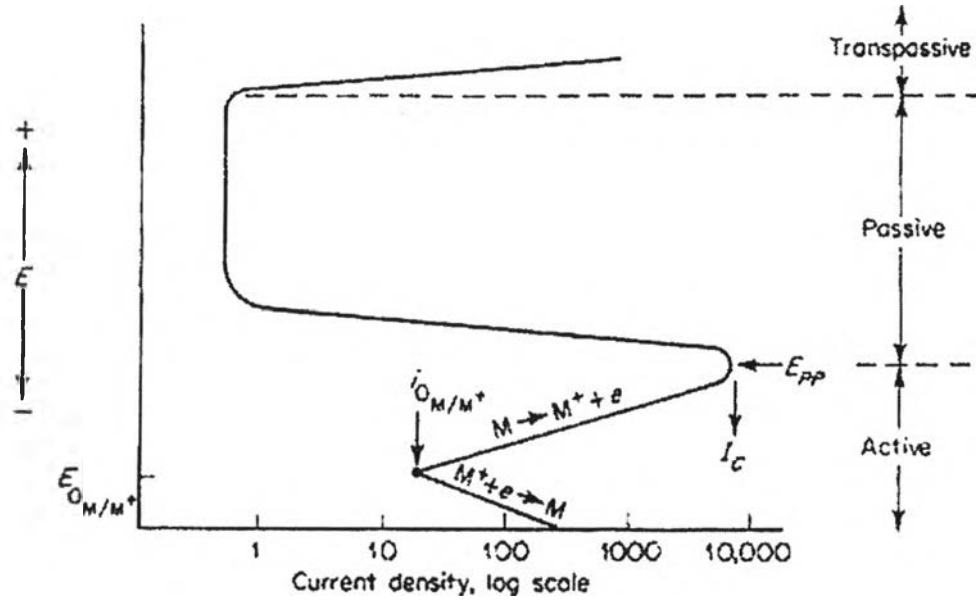

Figure 2.9 Typical anodic polarization curve of active-passive metal (Fontana, 1986).

In a system where the oxide film is already formed at the metal surface. The polarization will be different than in Figure 2.9. The existence of the oxide film can restrict the anodic dissolution or dissolution of metal ions through the oxide film. This is caused by the diffusion control of oxide film. This gives a plateau or steeper slope of the anodic polarization curve.

Sierra *et al* (2000) studied the electrochemical behavior of 1018 carbon steel in alkaline solution. They illustrated that the change in slope of anodic polarization over times resulted from the complicated oxidation process. In addition, the plateau indicated the presence of iron ions diffusion through the oxide film as shown in Figure 2.10

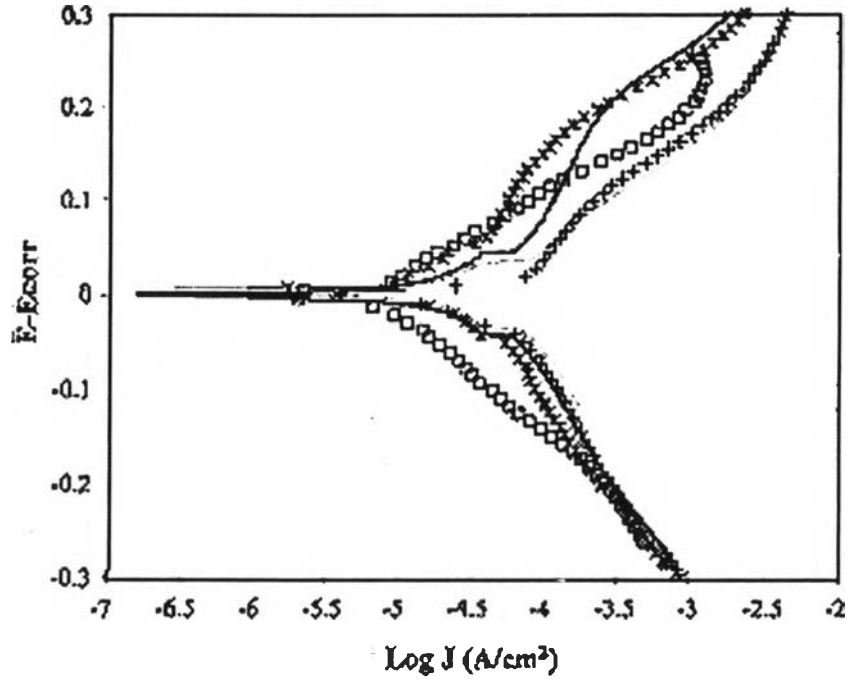

Figure 2.10 Anodic polarization curve obtained for 1018 carbon steel in alkaline sour environment (0.1 M $(NH_4)_2S$ and 10 ppm NaCN: pH 9.2), at scan rate of 1 mV/s. The immersion time was varied: open square, 0 h; asterisk, 3 h; thick solid line, 5 h; solid line 27 h; and multiplication sign, 79 h (Sierra *et al.*, 2000).

2.6.1 Mixed Potential Theory

As mentioned in section 2.6.2, such a system that has two or more oxidation-reduction reactions, the potential of each electrode will deviate from their equilibrium potential and cause the polarization. For instance, in the case of iron immersed in hydrochloric acid, the iron is rapidly corroded by hydrochloric acid, and the reaction occurring can be represented as in Figure 2.11.

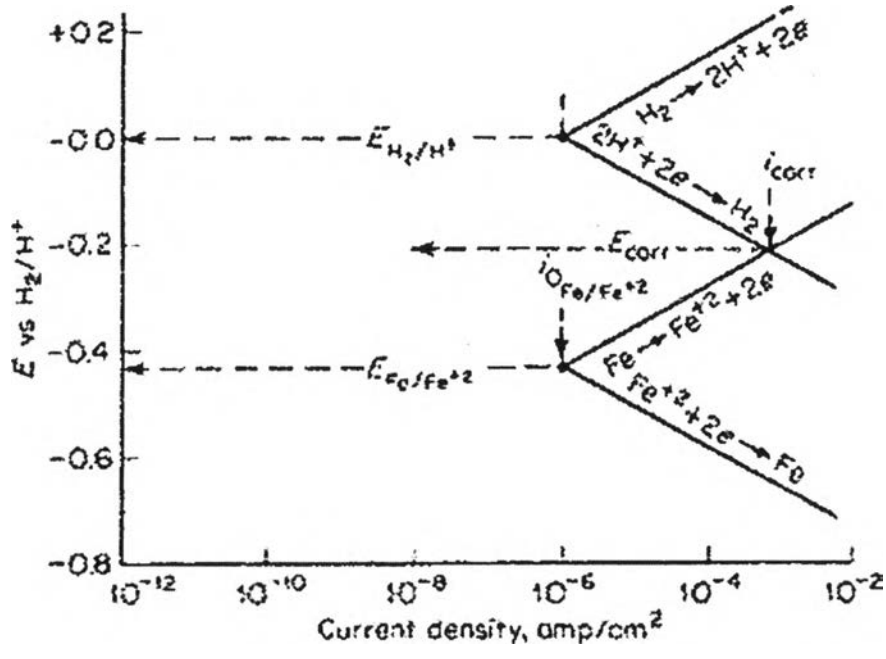

Figure 2.11 Schematic representation of electrode kinetic behavior of pure iron in acid solution (Fontana, 1986).

If one considers an iron electrode in equilibrium with its ions, it would be represented by an equilibrium potential ($E_{Fe/Fe2+}$) corresponding to the iron-iron ion electrode reaction and the corresponding exchange current density ($i_{0,Fe/Fe2+}$). Similarly, if one considers the hydrogen electrode reaction occurring on an iron surface under equilibrium conditions, then this particular equilibrium state would corresponding to an exchange current density ($i_{0,H+/H2}$) for this reaction on an iron surface. Certainly, the potential of each electrode cannot remain at their equilibrium potential according to the different Gibb free energies, and must locate at some potential at which the total rate of oxidation and reductions are equal. The potential at steady state where both total rates are equal is the intersection represented by a mixed or corrosion potential (E_{corr}) as shown in Figure 2.11. The current density corresponding to this potential is called corrosion current density (i_{corr}). At this steady state, it represents the dissolution rate of iron and the rate of hydrogen evolution. This value of i_{corr} can be applied to calculate the corrosion rate in the

system that consists of two or more electrodes. The corrosion rate can also be calculated by using an equation similar to Equation (2.22).

$$\text{Corrosion rate} = \frac{i_{corr}a}{nF} \qquad (2.23)$$

In order to construct the polarization curve, the electrochemical measurement needs to be set up. Figure 2.11 shows the configuration of three electrode cell that use for electrochemical measurement. A metal sample is immersed in the solution. The metal sample is called the working electrode (WE). Additional electrodes, a reference and counter electrodes, are also immersed in the solution. All electrodes are placed together in the three electrode cell compartment as shown in Figure 2.12

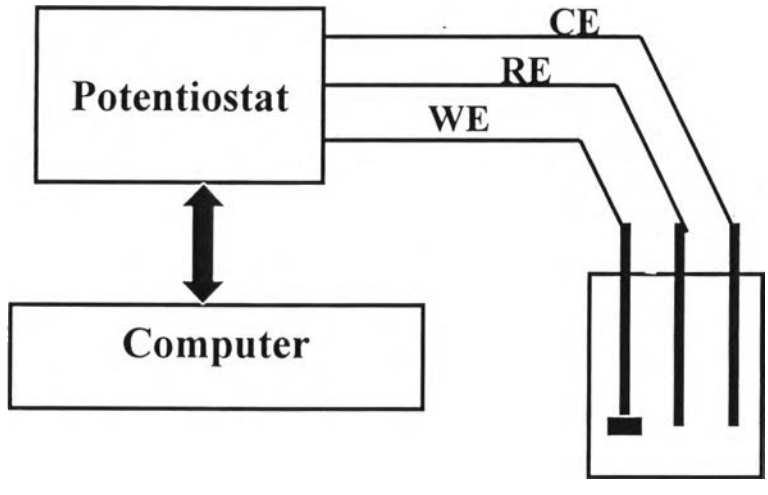

Figure 2.12 The configuration of three-electrode cell.

The counter electrode (CE) is an electrode that is used to make an electrical connection to the electrolyte solution so that a current can be applied to the working electrode. The processes occurring on the counter electrode are not important since it is usually made of inert materials (e.g., Pt) to avoid its dissolution.

The reference electrode (RE) is an electrode that is used as a reference point against the potential of the working electrode. The important properties of this electrode are always stable at its equilibrium potential or non-polarizable and highly reproducible potential.

All electrodes are connected to a device called a potentiostat. This allows the changing of the potential of the metal sample in a controlled manner while measuring the current as a function of potential. It should be noted that prior to the electrochemical test or no applied potential to the working electrode, the potential at this stage is called the open circuit potential (E_{oc}). In the ideal case, the values of E_{oc} and E_{corr} will, therefore, be identical when the equilibrium of the mixed potential electrode is achieved.

Figure 2.13 shows the typical polarization curve, when the scanning potential of the metal is performed with the potentiostat. The relationship between the potential and measured current density is a curved line at the region close to the E_{corr}. Since, the measured current density is the net current density, it accounts for both anodic and cathodic current. The net current density is related to the current densities of the electrochemical reactions occurring on the metal surface by the following equation.

$$i_{net} = i_{anode} - i_{cathode} \qquad (2.24)$$

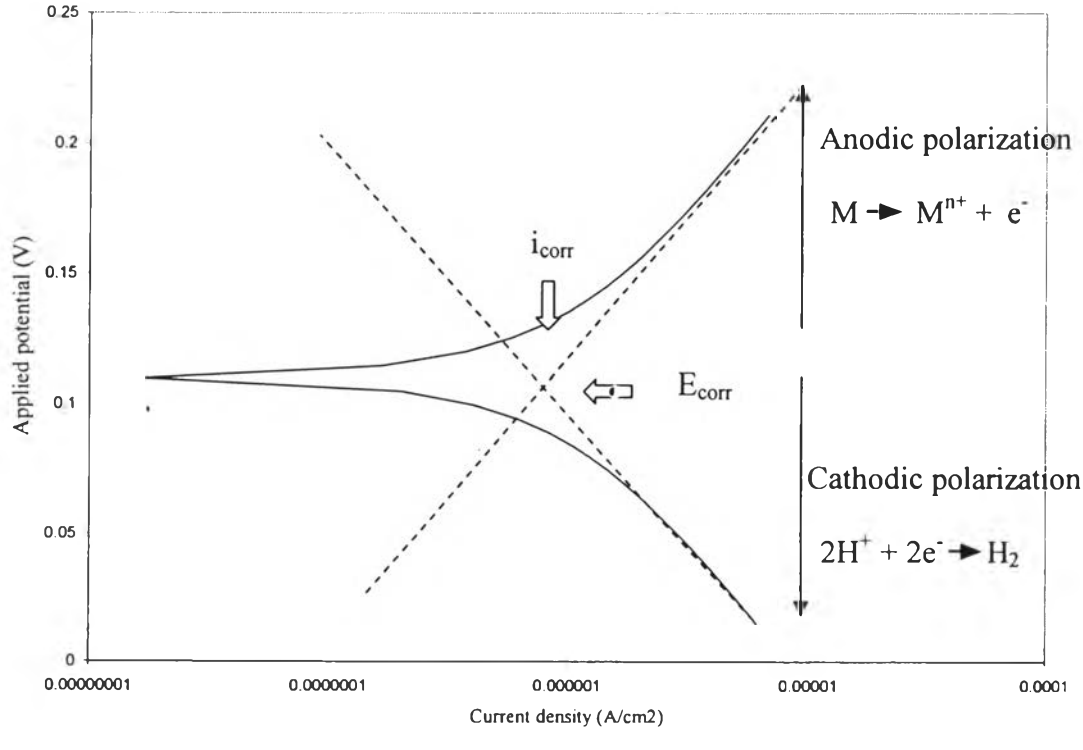

Figure 2.13 Schematic cathodic and anodic polarization curve.

The theoretical relationship between potential (E) and logarithmic of current density (i) is straight line as shown in the following equation.

$$E\text{-}E_{corr} = \pm \beta \log\left(\frac{i}{i_{corr}}\right) \qquad (2.25)$$

The sharp point in the curve is actually the point where the current changes signs as the reaction changes from anodic to cathodic or vise versa. The correspondence of the anodic and cathodic current density to the polarization curve can be expressed in the equation below

$$i_{anode} = I_{corr} \exp\left[\frac{2.303(E - E_{corr})}{\beta_a}\right] \qquad (2.26)$$

$$i_{cathode} = I_{corr} \exp\left[\frac{2.303(E - E_{corr})}{\beta_c}\right] \qquad (2.27)$$

The net current density in Eq (2.24), can be rearranged to

$$i_{net} = I_{corr}\left\{\exp\left[\frac{2.303(E - E_{corr})}{\beta_a}\right] - \exp\left[\frac{2.303(E - E_{corr})}{\beta_c}\right]\right\} \qquad (2.28)$$

Equation (2.28) is known as the Butler-Volmer equation. Where β_a is Anodic Tafel Slope and β_c is cathodic Tafel Slope. The exponential behavior of the current density with potential as related to Equation (2.28), means that the anodic contribution (First exponent term) to the net current density can generally be ignored if the potential is sufficiently more negative than E_{oc}, while the cathodic contribution (Second exponent term) can generally be neglected when the potential is significantly more positive than E_{oc}.

2.6.2 Electrochemical Impedance Spectroscopy

Based on the consideration, that the corrosion process is an electrochemical reaction in nature. It, therefore, involves electron transfer, which facilitates the dissolution of metal. If such a consideration can model this process, the corrosion can be predicted and control be facilitated. Electrochemical impedance spectroscopy (EIS) is one of the techniques, which has been widely used to study and characterizes passive films formed on metals or alloys. It attempts to explain the electrochemical or corrosion behavior by modeling with electrical circuit elements.

In principal, EIS work by applying the AC voltage (E) and measuring the current (I) response. The relationship between E and I can be presented as follows

$$E = IZ \qquad (2.29)$$

Impedance (Z) is the resistance of the system of interest and can be calculated from the above equation. Once, the impedance values are measured the AC circuit can be applied by fitting it with the electrical equivalent circuit elements such as a resistor, a capacitor and an inductor. The goal of the impedance technique is to measure the impedance and then to use the analogous circuit to model the measured impedance. The value of the resistance created by capacitors and inductors depend on frequency (f) while the value of resistance created by the resistor is independent of frequency.

When sinusoidal voltage is applied across the circuit composed only of a resistor, the resulting current is also a sine or cosine wave of the same frequency or no phase shift (ϕ) but different amplitude. If the circuit consists of capacitors and/or inductors, the resulting current will not differ only in amplitude but will also be phase shifted in time. This phenomenon is shown in Figure 2.14.

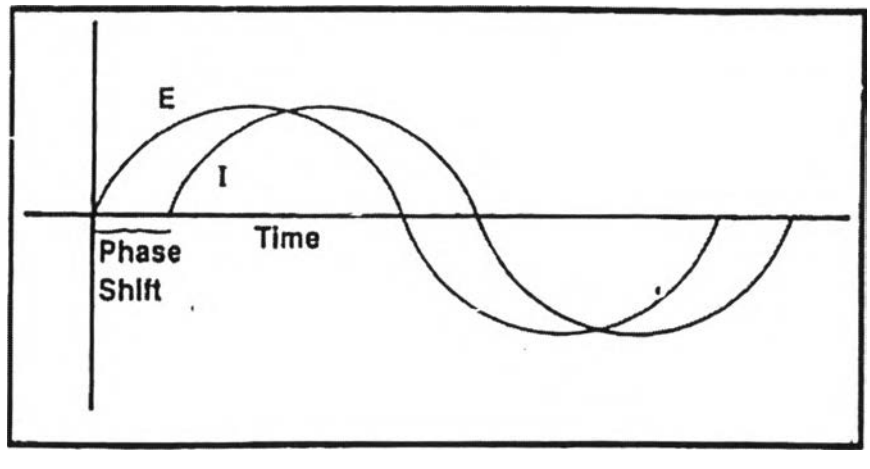

Figure 2.14 Sinusoidal AC voltage and current signals (Silverman, 1987).

The impedance analysis considers the voltage and current in vector representation instead of sinusoidal representation because of the ease for describing the analogous circuit in mathematical terms. A sinusoidal voltage and current can be depicted as a rotating vector as shown in Figure 2.15.

The current rotates at a constant angular velocity or ω (radian/s = 2πf). In Figure 2.15, the X component defines the observed current. Therefore, it becomes the real component of the rotating vector. The Y component is a contribution that is not observed. Therefore, it becomes an imaginary component. The mathematical convention for separating the real and imaginary components is to multiply the magnitude of the imaginary contribution by j and report real and imaginary values separately. The equation for AC impedance becomes

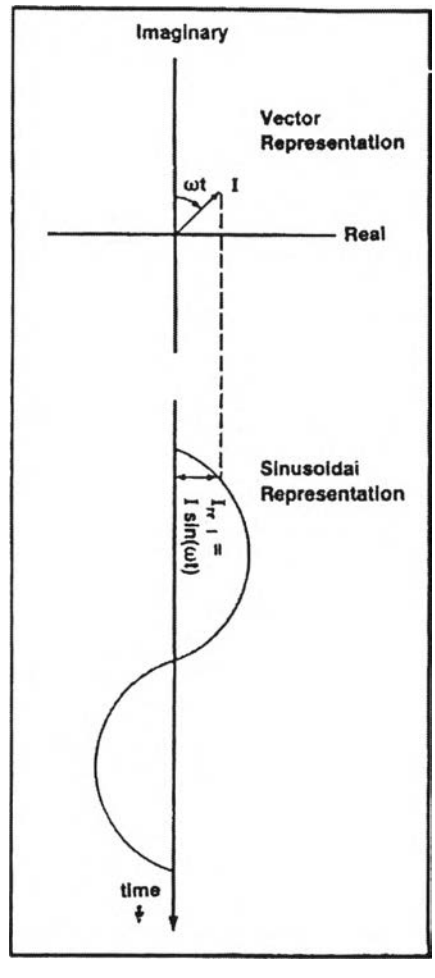

Figure 2.15 Relationship between sinusoidal AC current and rotating vector representation (Silverman, 1987).

$$E = E_{real} + E_{imaginary} = E' + jE'' \quad (2.30)$$

$$I = I_{real} + I_{imaginary} = I' + jI'' \quad (2.31)$$

Since, the linear relationship between the E and I, the impedance (Z) can be represented as

$$Z = \frac{E}{I} = \frac{E''+jE''}{I'+jI''} = Z' + jZ'' \quad (2.32)$$

The phase angle shift (ϕ) and magnitude or modulus of impedance can be calculated as the follow

$$\phi = \tan^{-1}\left(\frac{Z''}{Z'}\right) \quad (2.33)$$

$$|Z| = \sqrt{(Z')^2 + (Z'')^2} \quad (2.34)$$

In the corrosion process, if one can measure the Z' and Z" of the system of interest such as of the oxide film coated on the studied material, it provides the information to characterize the oxide film of such material.

2.6.2.1 Data Presentation

According to the impedance equation, the impedance variable can be presented in two different kinds of plots, Nyquist and Bode plot.

The Nyquist plot uses the expression of impedance that consist of the real (Z') and imaginary parts (Z"). The real part is plotted on the X-axis while the negative value of the imaginary contribution is plotted on the Y-axis. Each point on the Nyquist plot is the impedance at one frequency.

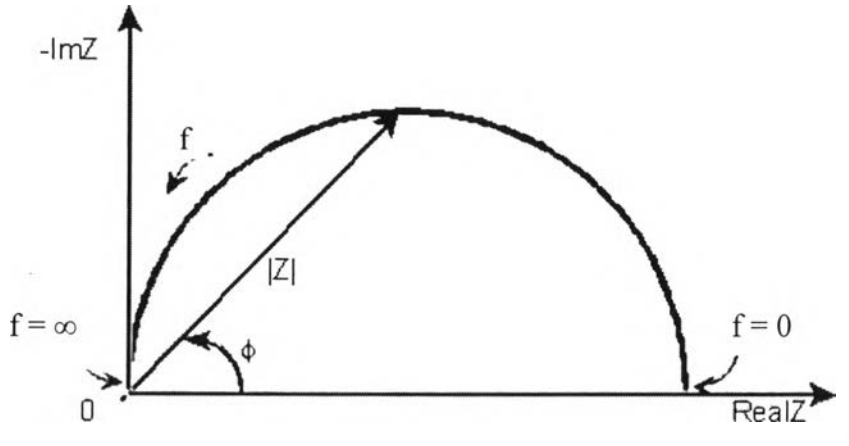

Figure 2.16 Nyquist plot with impedance vector.

Figure 2.16 has been annotated to show the low frequency data on the right side of the plot and high frequency on the left. In addition, the magnitude of impedance ($|Z|$) can be represented as the length of vector $|Z|$ from the point of origin. However, the major shortcoming of the Nyquist plot is the frequency presentation. It does not explicitly show the frequency at each point. The Nyquist plot in Figure 2.16 results from the electrical circuit of Figure 2.17. The semicircle is a characteristic of a single "time constant". The time constant is the multiplying result between resistance (R) and capacitance (C). The number of time constant normally corresponds to the number of parallel circuits between the resistor and the capacitor.

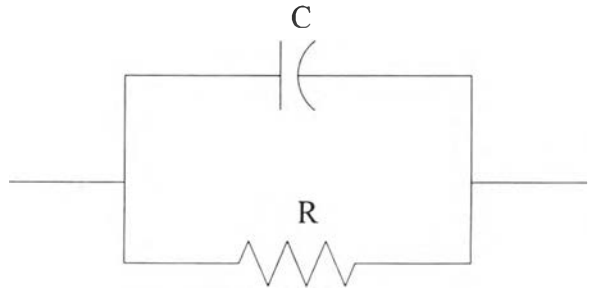

Figure 2.17 Analogous electrical circuit of Figure 2.16.

Another presentation is the Bode plot as presented in Figure 2.18. The impedance is plotted with the logarithm of frequency versus both the

magnitude of impedance ($|Z|$) and the phase shift. Unlike, the Nyquist plot, the Bode plot explicitly shows frequency information. The first information that can be extracted from the phase angle versus frequency curves is the number of distinguishable maxima or related shoulders. Each maxima or shoulder corresponds to a particular process that responds to the perturbing signal. The number of maxima or shoulder also corresponds to the number of the time constants. The appearance of the Bode plot can be used roughly for prediction the possible circuit model.

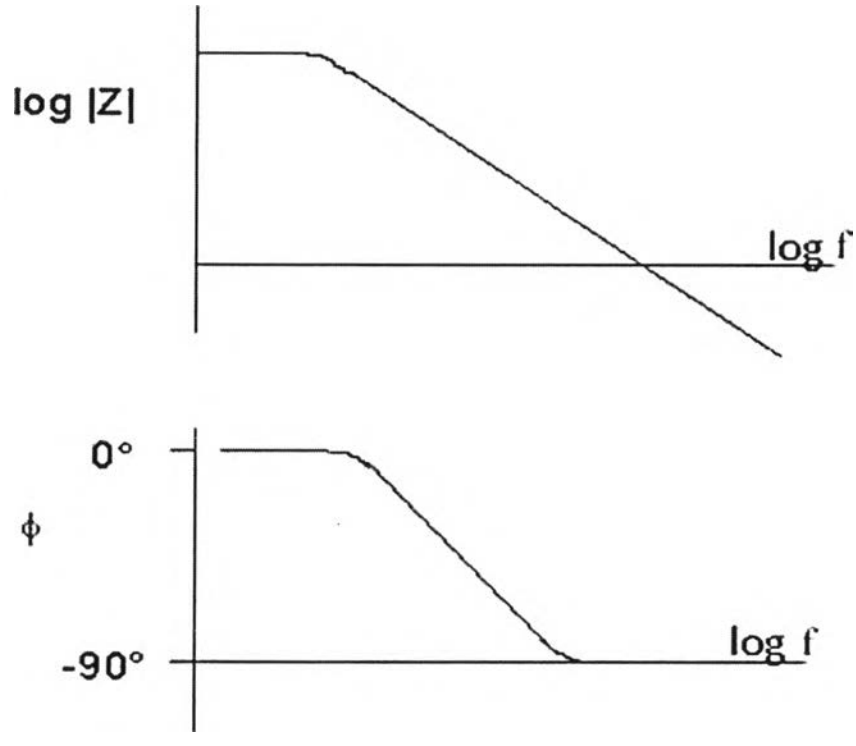

Figure 2.18 Bode plot with one time constant.

2.6.2.2 Physical Chemistry and Equivalent Circuit Element

a) Solution Resistance (R_s)

The solution resistance is often a significant factor in the impedance of an electrochemical cell. The resistance of the ionic solution depends on the ionic concentration, temperature and geometry of the area in which current is carried. The solution resistance (R_s) behaves like a resistor in the equivalent circuit element.

b) Charge Transfer Resistance (R_{ct})

The charge transfer means the transfer of metal ions into the solution, when the metal substrate is in contact with the electrolyte solution. The charge transfer reaction has a certain rate which depends on the kind of reaction, temperature, concentration of reaction products and potential. The charge transfer resistance (R_t) is defined as

$$R_{ct} = \frac{RT}{nFi} \qquad (2.35)$$

Where i = Exchange Current density

R = Gas constant

T = Absolute temperature

n = Number of electron involved

F = Faraday constant

The exchange current density can be calculated when R_{ct} is known. The exchange current density is proportional to the corrosion rate; consequently the value of R_{ct} can also reveal the corrosion rate. The higher value of R_{ct} means a lower value of corrosion rate and vice versa.

c) Double Layer Capacitance (C_{dl})

The double layer is created by the fact that the surface of metal in contact with the electrolyte solution. The metal surface has excess with electrons. Therefore, the counter ions in the solution can be attracted to the metal surface in order to neutralize the surface, resulting in the layer of two opposing charge. This structure response to AC voltage signal in a way is analogous to a capacitor as can be depicted in Figure 2.19.

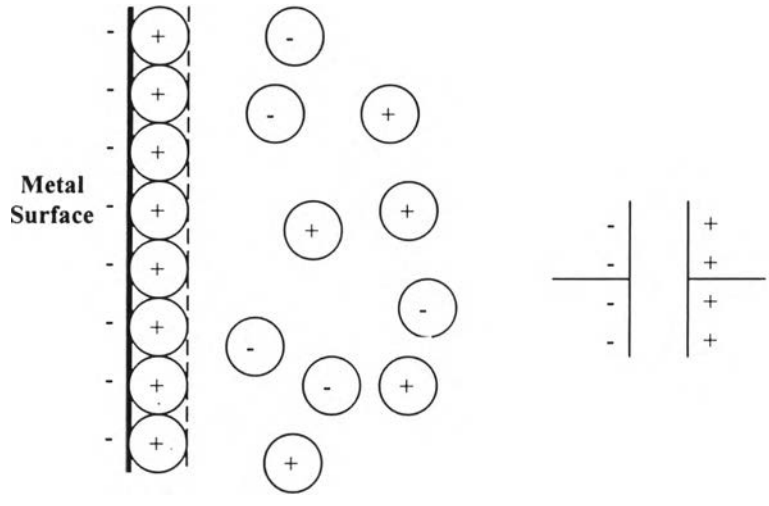

Figure 2.19 Schematic Diagram of Double layer capacitance.

d) Coating capacitance (C_f)

The Capacitor is formed when two conducting plates are separated by a non-conducting media, called the dielectric. The value of the capacitance depends on the size of plates, the distance between the plates and the properties of the dielectric. The relationship is

$$C_f = \frac{\varepsilon_o \varepsilon A}{d} \qquad (2.36)$$

Where $\varepsilon_o = 8.85 \times 10^{-14}$ F/cm

ε = dielectric constant

A = surface of one plate

d = coating thickness

Based on the Eq (2.36), it revealed that the coating thickness can be calculated if the value of C_f is available. However, the value of ε depends on the material. The different composition gives different values of ε. This value is sensitive to the water uptake, resulting in higher capacitance. However, the value of ε is not extensively reported.

2.6.2.3 Common Equivalent Circuit Models

a) Randles Cell

The Randles is one of the simplest and most common cell models. It includes the R_s, C_{dl} and R_{ct}. The equivalent circuit for the Randles cell is shown in Figure 2.20. The double layer capacitance is in parallel with the impedance due to the charge transfer resistance.

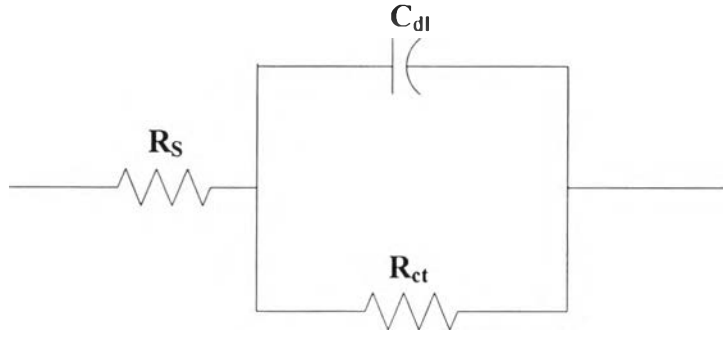

Figure 2.20 Equivalent circuit of Randles cell.

Figure 2.21 is the Nyquist plot for a typical Randles cell. The Nyquist plot for the Randles cell is always a semicircle. The solution resistance R_s can found by reading the real axis at the high frequency intercept. The real axis value at low frequency is the sum of charge transfer resistance (R_{ct}). The diameter of the semicircle is, therefore, equal to the R_{ct}.

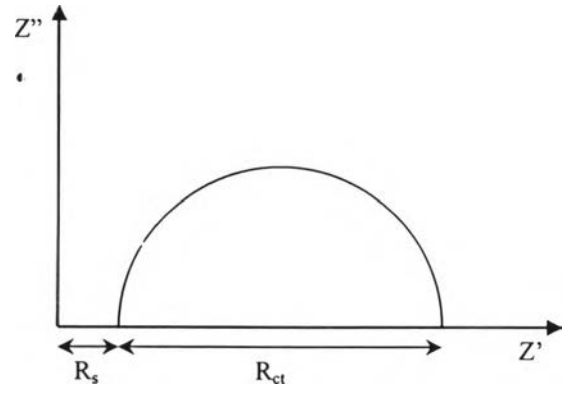

Figure 2.21 Nyquist plot of Randles cell for metal undergoing uniform corrosion rate.

Figure 2.22 is the Bode plot. R_s and the sum of R_S and R_{ct} can be read from the magnitude ($|Z|$) plot. The one shoulder of phase shift plot corresponds to one semicircle obtained on the Nyquist plot, which is called a single time constant.

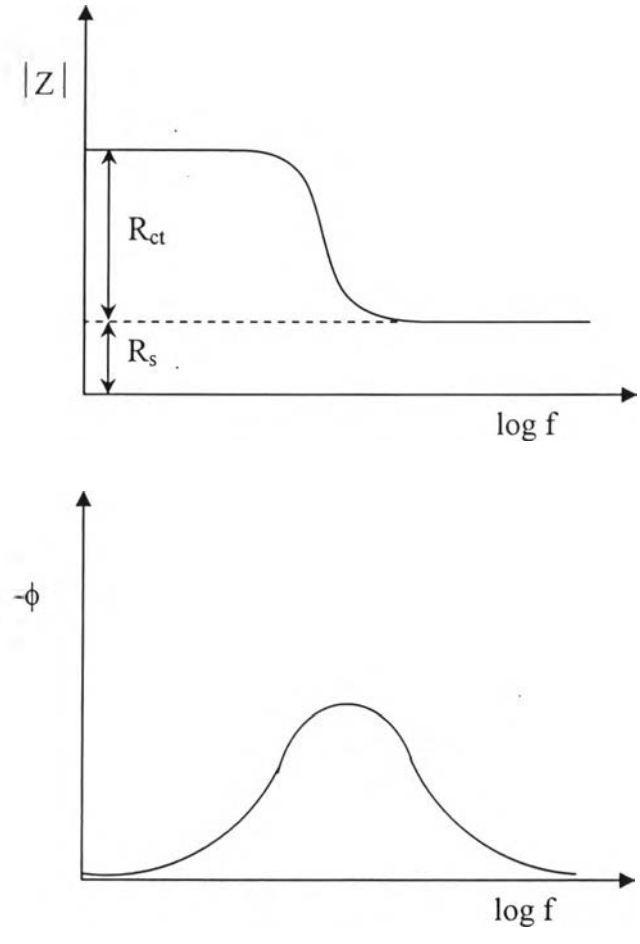

Figure 2.22 Bode plot of Randles cell for metal undergoing uniform corrosion rate.

b) Coated Metal Cell

Most coatings degrade with time, resulting in more complex behavior. After a certain amount of time, solution can penetrate into the coating and form a new liquid/ metal interface under the coating or form a double layer capacitance (C_{dl}). Corrosion phenomena can occur at the new interface. The capacitance of the intact coating is represented by C_f. Its value is much smaller than

a typical double layer capacitance (C_{dl}). Its units are pF or nF. R_f is coating resistance or pore resistance. It is the resistance of the ion conducting paths that develop in the coating. These paths may not be physical pores filled with solution.

On the metal side of the pore, this model assumes that an area of the coating has delaminated and a pocket filled with the solution has formed. This solution can be very different from the bulk solution outside the coating. The interface between this pocket of solution and the bare metal is modeled as C_{dl} in parallel with a kinetically controlled charge transfer reaction. The equivalent circuit of this model is shown in Figure 2.23.

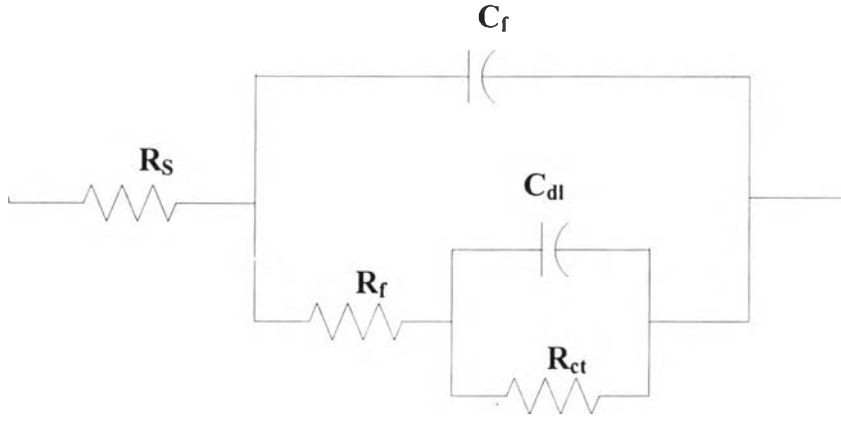

Figure 2.23 Equivalent circuit of coated metal.

When data fitting with equivalent is achieved, it can provide an estimated value of R_s, R_{ct}, R_f, C_{dl} and C_f. The inverse value of R_{ct} and R_f can refer to the corrosion rate and coating porosity, respectively. The Nyquist plot of this model is shown in Figure 2.24. The Bode plot of the same model is shown in Figure 2.25. The two time constants are visible as presented in the form of two semicircles in the Nyquist plot and two shoulders in the Bode plot.

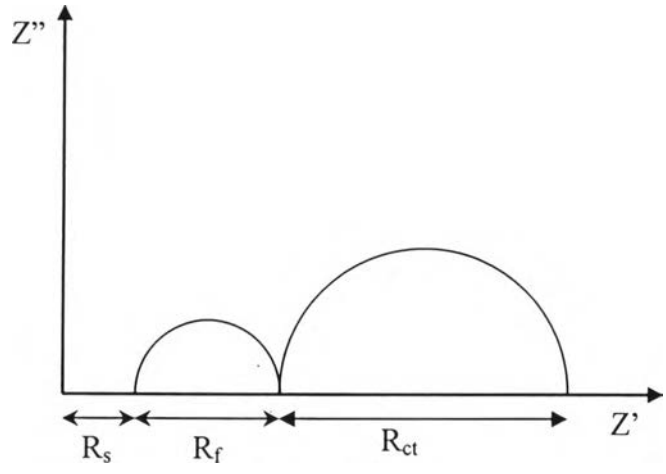

Figure 2.24 Nyquist plot for coated metal.

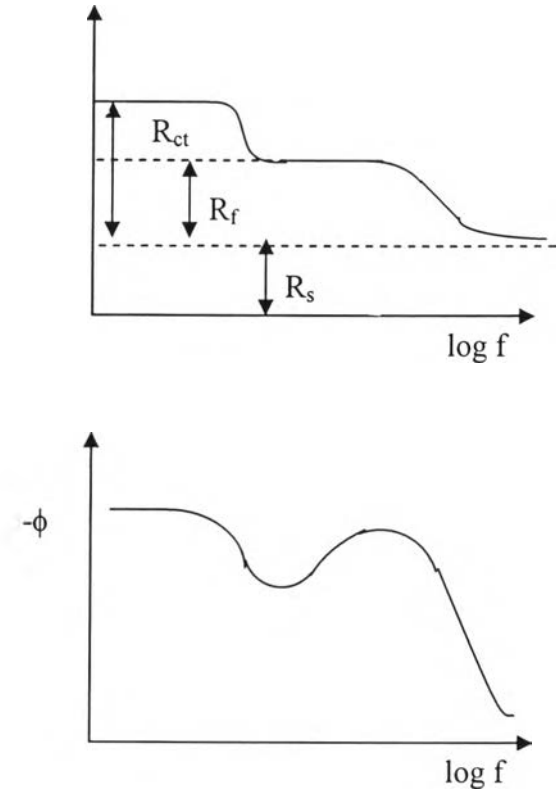

Figure 2.25 Bode plot for coated metal.